UNDERWATER ACOUSTIC COMMUNICATION CHANNEL CHARACTERIZATION AT LOW FREQUENCIES IN SHALLOW WATER

J. B. Franklin (1), & P. J. Barry (1)

(1) Defence Research Establishment Atlantic, P. O. Box 1012, Dartmouth, NS, B2Y 3Z7, Canada.

ABSTRACT

The channel characteristics for sound propagating at 1100 Hz off Nova Scotia, Canada in winter conditions were measured at a shallow water station over Sable Bank. Experimental and model results for propagation loss and time spreading are compared at source-receiver separations out to 180 kilometers. Relatively little time spreading was observed which is consistent with propagation dominated by a small number of modes. The low propagation losses observed are attributed to low bottom losses. The data were gathered using mobile platforms. The observed frequency spreading (typically 0.25 Hz) is attributed to platform motion excited by motion of the sea surface. The applicable propagation parameters are used to predict the channel capacity of a Differential Quadrature Phase Shift Keying communication system operating in the same environment and using a vertical receiving array to provide modal decomposition (mode filtering). The issue of providing sufficient transmitter power to meet a specific error rate specification is also addressed.

1. INTRODUCTION

Time and frequency spreading of signals and the propagation loss between the transmitter and the receiver are important environmental inputs to the design of a high capacity long range underwater acoustic communication channel. These parameters impact directly on the required transmitter power and on the maximum achievable data rate. Propagation processes vary widely with location and conditions. In this paper we confine our interest to the propagation of signals at a shallow water site exhibiting a low loss bottom and isothermal water.

Underwater communications out to 200 kilometers should be operated at low frequency if power demands for the transmitter are to be kept reasonable. Operation at low frequency raises issues regarding transmitter bandwidth (and therefore data rate) because, for a typical wide-bandwidth projector having a bandwidth extending over one frequency octave, the transmitter bandwidth is proportional to the operating frequency. Choosing a modulation scheme which maximizes the bandwidth efficiency (data rate in bits per second divided by the bandwidth in Hz) is consequently very important.

CHANNEL CHARACTERISTICS

The main thrust of this paper is to describe the channel characteristics which affect the performance of underwater acoustic communications. Frequency spreading, time spreading, and propagation loss are described for a particular environment, namely, a shallow water site over Sable Bank off Nova Scotia in winter conditions. The experimental results are compared to model predictions and used to predict the performance of an underwater acoustic communication system having a bandwidth covering 800 to 1600 Hz.

2. PROPAGATION LOSS MEASUREMENTS

Propagation loss measurements were carried out using two ships opening one another at a combined speed of 26 knots. Source signals were provided by 0.8 kg TNT charges detonated at a depth of 18 m. The charges were dropped at range intervals of approximately 2.4 km by one of the ships, and the signals were received on an omnidirectional hydrophone in a horizontal line array towed by the second ship. The bathymetry for the propagation run is shown in Figure 1. The opening run commenced with both ships at near zero range on the graph and the ships opened on reciprocal courses. The receiving ship opened to the left (in the direction of negative range) at 10 knots, and the source ship opened to the right (in the direction of positive range) at 16 knots. The water depth was relatively constant over the source ship's track. However, the water depth increased significantly over the receiving ship's track. Isothermal water conditions (1.5° C; sound speed--1455 m/s) existed throughout the water column and the wind speed varied between 10 and 15 knots. The bottom consisted of a mixture of sand and gravel. The bottom density was 2000 kg/m^3, the sound speed in the bottom was 1710 m/s, and the attenuation of sound in the ocean bottom was 0.75 dB per wavelength[1].

The received signals were filtered in a band 440 Hz wide centered at 1119 Hz, squared, and integrated to obtain the total received energy. The source energy in this frequency band for this charge weight is 219.1 dB re 1 μPa^{2}s.

The measured propagation loss data as a function of range are shown in Figure 2. Propagation losses are low. The KRAKEN normal mode propagation model[2] was used to predict propagation loss in the conditions of the experiment. Attenuation due to sound absorption was computed using the Global Model for Sound Absorption in Sea Water[3] for pH=8.27 (0.13 dB/km at 1100 Hz). Mode 1 is the mode with the least propagation loss. Modes 2 and 3 exhibited losses which were about 6 dB greater than that of mode 1. Modes 1 to 3 accounted for nearly all of the received energy. The propagation loss for the incoherent sum of the first 8 modes is in very good agreement with the experimental results. The model results in Figure 2 are approximate because the model was run for a constant water depth of 55 m. Moreover no attempt was made to take into account the conversion of energy from a low order mode to higher order modes via scattering at slightly rough boundaries.

CHANNEL CHARACTERISTICS

The depth of water at the source, which was opening at 16 knots varied between 40 and 55 m over the propagation run and the water depth at the receiver varied from 45 to 97 m over the run. (See Figure 1.) The depth variation is however very slow so that the modes can be considered to be uncoupled and adiabatic mode theory can be used. With this assumption, a given mode can be considered to adjust to the varying conditions of the waveguide (depth variation). Attenuation will continue to be dominated by absorption. However, the response functions of the source and receiver change as the depth of water under the source and receiver changes. This will result in a variation in the contributions for the different modes from those estimated for a constant water depth of 55 m.

The KRAKEN model is not well suited to a geometry where both the source and receiver are moving and the bathymetry is changing. However the KRAKEN model was run at 9 source-receiver separations each with the correct bathymetry for that range. The model was run at 14.3, 38.5, 62.6, 86.8, 98.7, 120.6, 147.2 159.3 and 169.5 km source-receiver separations. The propagation loss results so obtained were found to be in good agreement with the constant depth estimates of Figure 2 except at the longest range where the stronger contribution of mode 2 predicted lower propagation loss.

Underwater communications must take account of signal fading. Since more than a single mode contributes to the signal energy, the potential exists for fading and signal reinforcement associated with the coherent addition of the modes. The incoherent addition of mode energy in Figure 2 cannot show this effect. Neither do the experimental data because of considerable averaging in the frequency domain (440 Hz). The KRAKEN propagation model results for 1119 Hz which take into account the coherent combination of the mode energies are shown in Figure 3. Note that the peak-to-peak amplitude of the fluctuations is about 10 dB and that several deep fades are in evidence.

Experimental results for fading were also obtained. A CW signal 50 seconds long was transmitted by an electroacoustic projector suspended from a drifting ship using a suspension system to isolate the projector motion from that of the surface vessel and the sea surface. The signal was received by a single omnidirectional hydrophone in a horizontal line array which was towed by a second vessel which closed the projector at a speed of 10 knots. The received signal was complex heterodyned down to a much lower frequency for analysis. The real part of the heterodyned signal is shown in Figure 4 for a source-receiver separation of 42 km. Fluctuations in the amplitude extending from 0.3 to 0.5 volts are in evidence (~4.4 dB). The amplitude structure can be expected to vary with frequency, horizontal separation between the source and receiver, and the depths of the transmitter and receiver. The use of depth diversity at the receiver is a relatively simple method to avoid the degradation in signal-to-noise ratio brought about by deep fades. Even more attractive is the use of a vertical array of hydrophones to coherently process the signals to steer beams for each of the low order modes[4] (mode filtering). Such an approach is more reliable than depth diversity, and it provides a spatial gain against ambient noise. Diversity selection would still be employed to select

the best beams (modes) because mode excitation at the transmitter is not necessarily known. The beams so selected would then be incoherently combined to obtain further processing gains.

3. TIME SPREADING OF 1100 HZ SIGNALS

The explosive charges used to measure propagation loss were also used to measure time spreading. The received signals were processed by a circuit comprising a bandpass filter with a bandwidth of 440 Hz and a center frequency of 1119 Hz, followed by a squarer and a single pole low pass filter. The low pass filter which was used to attenuate the ripple associated with the squaring of the band limited signal had a time constant of 0.61 ms. The total integration time of this circuit was found to be 2 ms.

A typical output of the circuit is shown in Figure 5 for source-receiver separation of 118 km. The low pass filter cut-off frequency was set as high as possible to maintain temporal resolution. Therefore, some ripple at twice the center frequency of the bandpass filter is in evidence. Time spreads were taken to the 6 dB down points from the peak power level. At the range shown in Figure 5, a single arrival is shown to dominate the time record. The time spread is close to the integration time of the processing circuit.

Another example at a source-receiver separation of 56 km is shown in Figure 6. The arrival structure for this record clearly shows two distinct arrivals separated by about 7 ms. The measured time spread at the 6 dB down points includes both arrivals and is found to be 9 ms. Figure 7 shows a succession of arrivals extending over 26 ms, not all of which are shown. The character of this pulse differs significantly from the arrival structures in Figures 5 and 6 and illustrates an unfavorable condition for an underwater acoustic communication system. The use of a vertical array of hydrophones to focus on the low order modes of interest should reduce the time spreading shown in Figure 7.

The measured values of time spreading versus range are shown in Figure 8. At the beginning of the run there is considerable time spreading indicating that there were contributions from both low and high order modes. However, out to 80 km most of the signals in the frequency band of interest are spread less than 10 ms. Some of the signals show time spreading close to the integration time of the circuit indicating that the dominant contribution is from a single mode.

The time spread between the first and second modes obtained using the KRAKEN shallow water propagation model which includes the variable bathymetry is represented by the solid line in Figure 8. Given two mode arrivals, this curve sets the envelope for the minimum time spread. Given a single dominant mode, the resolution of the processing circuit (2 ms) provides the envelope for the minima of the data (not shown in Figure 8). Greater time differences can of course occur when more than two modes generate significant contributions or when the dominant modes are of higher

order. (See for example, the time difference for mode arrivals 1 and 3 shown in dashed line in Figure 8.)

4. FREQUENCY SPREADING OF 1100 HZ SIGNALS

Frequency spreading of 50-second rectangular-envelope 1100 Hz center-frequency signals was examined as a function of range at the Sable Bank location. A free-flooding ring projector deployed at a depth of 35 m from a drifting ship was used to generate these signals. A suspension system was used to isolate the projector from the motion of the sea surface and the vessel to which it was tethered. The signals were received on a single omnidirectional hydrophone in a towed array which closed range to the transmitter at a speed of 10 knots. These measurements were made immediately before the propagation loss experiments were carried out. The water depth was 55 m, and the wind speed was 10-15 knots. The data were processed using a resolution of 0.075 Hz, 3 averages, a Hanning window, and 50% overlap. The frequency spread was measured to the 6 dB down points. The frequency spreads at the ranges for which measurements were obtained are shown in Figure 9. Taking the coherence time to be the reciprocal of the frequency spread, we find that the coherence times range from 4 to 6 seconds for the transmitter-receiver separations investigated.

A more detailed look at phase coherence is required to design a Differential M-ary Phase Shift Keying (DMPSK) communications system. Estimates for the phase of the CW pulse shown in Figure 4 for a source-receiver separation of 42 km were obtained using the real and imaginary components of the heterodyned signal. The resulting phase data were next unwrapped and finally the linear trend in the unwrapped data was removed. The results are shown in Figure 10. The phase variation is shown to be periodic having a peak amplitude of about 2.8 radians and a period of about 14 seconds. This relatively long period for the phase fluctuations is unlikely attributable to scattering at the sea surface. We have therefore attributed the cause of phase fluctuations to platform motion. In other records, the period of the phase was smaller and was found to correspond to the swell period. This behavior is attributed to surge and depth variations of the receiving array as the towing vessel closed range to the transmitter.

The steepest slope for the record in Figure 10 and indeed for the other phase records examined is less that 1.5 radians per second, which corresponds to a peak Doppler of 0.6 knots. Phase information is required in a differential M-ary PSK system to determine the minimum symbol repetition rate. For example if the symbol duration is 0.1 sec, Figure 10 shows a maximum phase error of .15 radians from one symbol to the next. Reduction in the amplitude of the phase fluctuations is expected if both the transmitter and the receiver can be made quasi-stationary.

5. COMMUNICATION SYSTEM DESIGN

The propagation measurements in the previous section show that the channel is highly underspread. In other words, the reciprocal of the frequency spread is much greater than the time spread. DMPSK is therefore well suited to this environment and presents the opportunity to maximize bandwidth efficiency[5]. A vertical receiving array with sufficient aperture should help alleviate fading. However, unless sophisticated equalization is used, it is not expected that the suppression of unwanted modes by the receiving array can adequately reduce intersymbol interference so that very short pulses matched to the projector bandwidth can be used. For the purposes of this paper we take a conservative approach in which a relatively long pulse length is used (significantly greater than the time spread in the channel). Narrowband channels would therefore be required. Relative to a single broadband channel, the use of a narrowband channel would avoid some of the difficulties associated with mode steering over an octave band as well as the effect of the projector frequency response on the pulse shape. Multichannel operation is consequently required if the entire bandwidth of the transmitter is to be used. Intersymbol interference suppression must therefore address the frequency separation of channels as well as the time separation of pulses. The main tenets of the design philosophy for the communication system are as follows:

i) Mode filtering using a vertical array of sensors at the receiver followed up by diversity selection of the best beams (modes) is specified. This procedure should eliminate deep fades in the signal strength and obtain a significant spatial processing gain against ambient noise.

ii) A CW pulse with a Hanning window applied is used to represent each symbol. The low spectral sidelobes for this pulse type are well suited to reduction of intersymbol interference between channels. The pulse duration, T, is set at 100 ms which is significantly greater than the time spread of the experimental results at all ranges. The receiver performance is consequently dominated by the signal characteristics at all ranges. Over this time interval there is negligible temporal decorrelation of the signal.

iii) Acceptable intersymbol interference within each channel should be achieved using a pulse repetition rate of T^{-1} (10 symbols per second). There is no overlap of the transmitted CW pulses.

iv) Differential QPSK modulation is specified.

v) Negligible intersymbol interference between channels should be achieved using a frequency separation of 2.5/T (25 Hz) and interleaving the pulses in the time sequence for adjacent channels. This action reduces the transmitter peak power requirement. The bandwidth extends from 800 to 1600 Hz. The resulting 32 channels yield an overall data rate of 320 symbols/s (640 bits/s).

vi) The receive filters are matched to the transmitted pulse.

CHANNEL CHARACTERISTICS

The error rate introduced by additive Gaussian white noise should be maintained at a very small value. The ratio of energy per symbol to the ambient noise spectrum level at the output of the matched filters (E_s/N_o) was accordingly set at 16 dB. Note that there are 2 bits per symbol for QPSK modulation. The corresponding bit error rate of 10^{-6} assumes no processing gain due to the incoherent combination of the individual modes[6]. Since the concept under consideration in this paper can take advantage of this feature, an even lower error rate should obtain.

The source level required to maintain the specified signal-to-noise ratio was calculated using the highest propagation loss of those shown for modes 1, 2, and 3 in Figure 2 at a range of 170 kilometers. This propagation loss (TL) is 110 dB, and the resulting peak symbol source level required for each channel is given by

$$SL = (E_s/N_o) - 10 \text{ Log } T + TL + N_o + 4.3 - AG$$

$$= 195.3 \text{ dB re } 1 \mu\text{Pa at } 1\text{m.} \qquad (1)$$

Equation (1) assumes that the ambient noise spectrum level (N_o) is 65 dB re 1 $\mu Pa^2 s$ (as measured during the experiment). The constant, 4.3 dB, takes into account the fact that the ratio of the pulse energy to the peak source level at the transmitter for each pulse is 0.375. An array gain (AG) of 10 dB is assumed. Note that the composite propagation loss which includes all modes cannot be used because the receiving array separates out the low order modes.

The projector is assumed to be pressure amplitude limited. Since the Hanning-windowed pulses on alternate channels are interleaved in the time sequence, the overall source level is based on simultaneous transmissions on only 16 channels. The resulting total peak rms source level becomes

$$SL_{total} = 195.3 + 20 \text{ Log}(16)$$

$$= 219.4 \text{ dB re } 1 \mu\text{Pa at } 1\text{m.} \qquad (2)$$

If a capability only out to 85 kilometers is required, this source level can be reduced by about 15 dB.

There is scope to increase the capacity of the channel given the same 800 Hz bandwidth. Single channel operation using a very short pulse duration (~ 800 symbols/s yielding 1600 bits/s) has been mentioned above. Adaptive equalization and training sequences would undoubtedly be required using this approach[7]. This approach would reduce the peak rms source level required of the transmitter because provision for the peak transmitter power requirement is limited to a single channel. The single channel concept would of course require greater power (4 dB) because the data rate is higher. Simple equalization should also be explored for application to the multichannel concept to increase the pulse repetition rate and/or to decrease the frequency separation of channels.

7. CONCLUSIONS

Frequency and time spreading measurements at a site over the Sable Bank in winter conditions showed a highly underspread channel. Even with mobile platforms, the frequency spread was very small. Time spreading was attributed to a sequence of mode arrivals—a sequence which was usually limited to contributions from one or more of the first three modes. Propagation loss was relatively low in the conditions of the experiment—isothermal water and low loss bottom. However, at the longer ranges losses up to 110 dB for the low order modes were in evidence. A concept for a communications link was advanced in which we proposed a vertical array of sensors to act as a mode filter at the receiver to reduce the effects of time spreading at the array output with particular interest in avoiding deep signal fades. Being concerned that the rejection of other modes by this spatial filter might be insufficient to control intersymbol interference we proposed a multichannel telemetry system which specified a symbol duration significantly greater than the measured time spread. Performance estimates for the proposed Differential QPSK communication system at 170 km showed a capacity of 640 bits/s and a transmitter source level requirement of 219.4 dB re 1 μPa at 1m.

8. REFERENCES

[1] Alisdair Mckay, "Compressional Wave Measurements in the Surficial Sediments of Sable Island Bank", Nova Scotia Research Foundation, Dartmouth, N.S., DREA CR 85/404.

[2] M. Porter, "The KRAKEN Normal Mode Program", SACLANTCEN Memorandum SM-245, September, 1991.

[3] R.H. Mellen, P.M. Scheifele, and D.G. Browning, "Global Model for Sound Absorption in Sea Water", Naval Underwater Systems Center, Newport, Rhode Island, 1987.

[4] T.C. Yang, "A method of range and depth estimation by modal decomposition", J. Acoust. Soc. Am. 82 (5), November 1987, 1736-1745.

[5] Simon Haykin, "Digital Communications", John Wiley and Sons, 1988, p. 332.

[6] J.C. Bic, D. Duponteil, and J.C. Imbeaux, "Elements of Digital Communication", John Wiley and Sons, 1991, p. 218.

[7] M. Stojanovic, J. Catipovic, J.G. Proakis, "Adaptive multichannel combining and equalization for underwater acoustic communications", J. Acoust. Soc. Am. 94 (3), September, 1993, 11621-1631.

CHANNEL CHARACTERISTICS

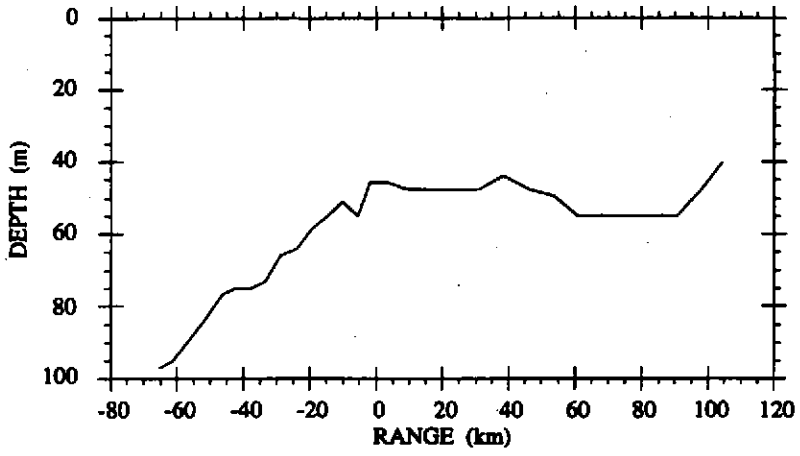

Figure 1: Bathymetry for the propagation loss measurements.

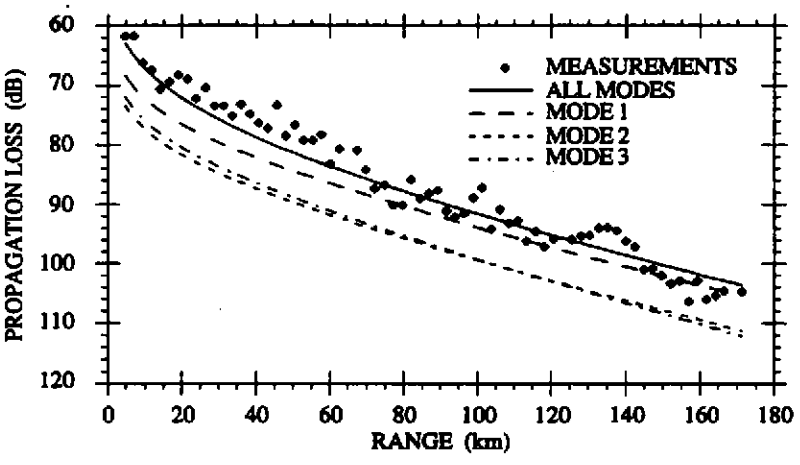

Figure 2: Measured propagation loss, estimates of propagation loss for the incoherent sum of all the significant modes and modes 1, 2 and 3 calculated using the KRAKEN normal mode model at 1119 Hz.

CHANNEL CHARACTERISTICS

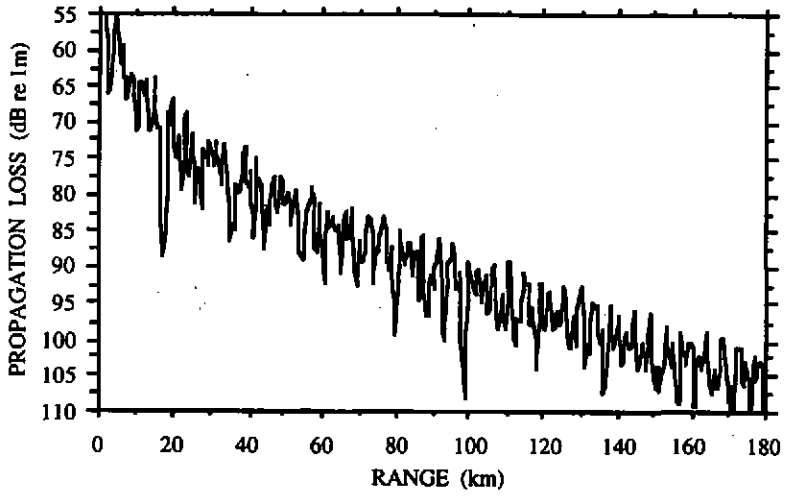

Figure 3: **Coherent propagation loss versus range at 1119 Hz, as estimated by the KRAKEN normal mode model for isothermal water with a constant water depth of 54.86 m.**

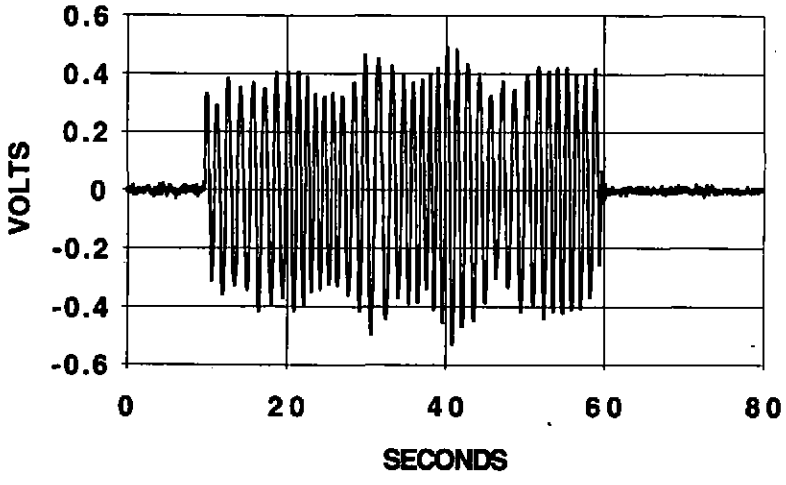

Figure 4: **Signal amplitude for CW pulse at 1100 Hz at a source-receiver separation of 42 km.**

CHANNEL CHARACTERISTICS

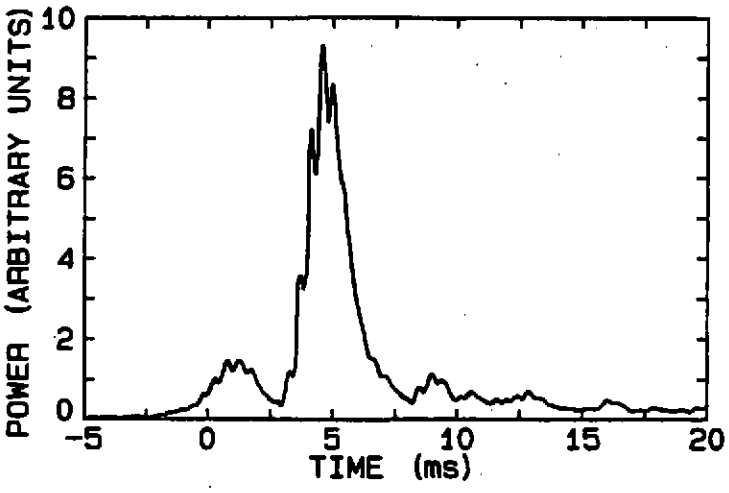

Figure 5: Pulse arrival structure at a source-receiver separation of 118 km.

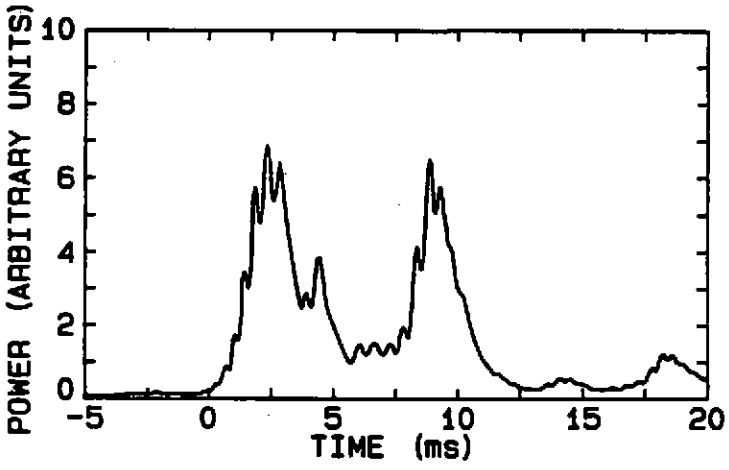

Figure 6: Pulse arrival structure at a source-receiver separation of 56 km.

CHANNEL CHARACTERISTICS

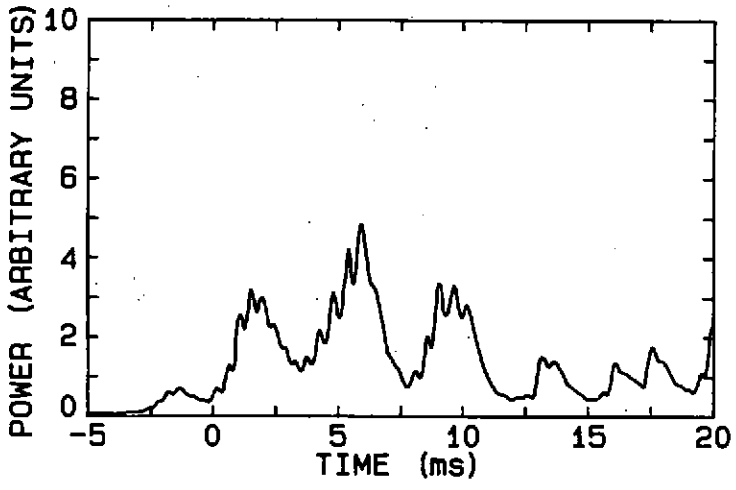

Figure 7: Pulse arrival structure at a source-receiver separation of 120 km.

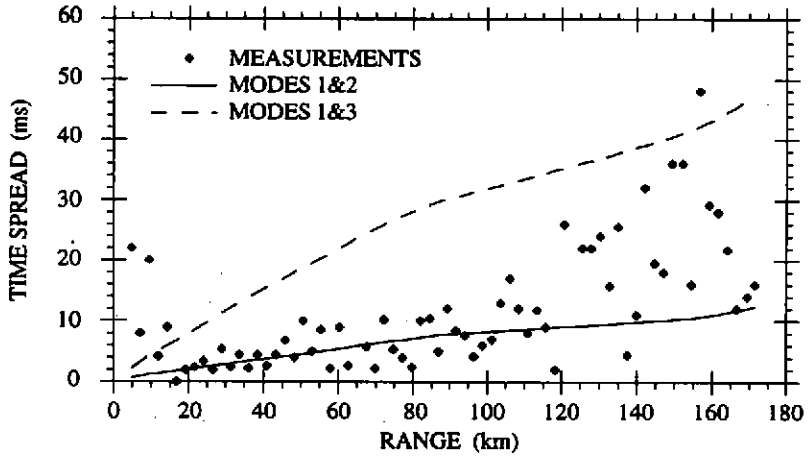

Figure 8: Time spread versus range for different modes at 1119 Hz.

CHANNEL CHARACTERISTICS

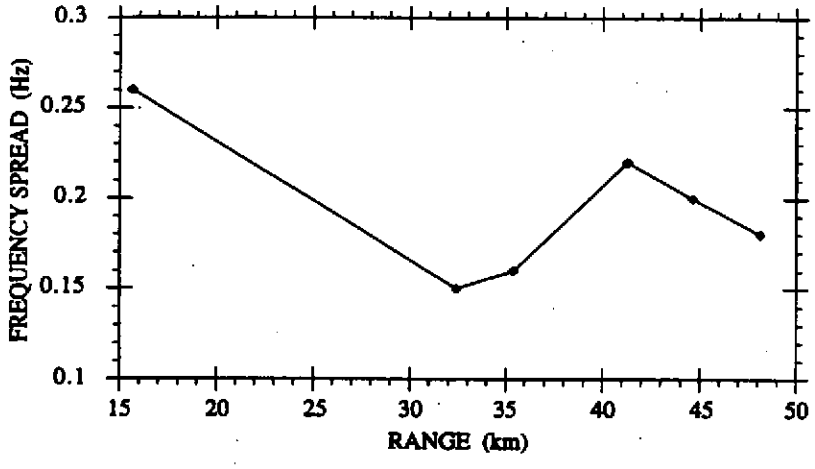

Figure 9: Frequency spreading versus range (wind speed 10-15 knots).

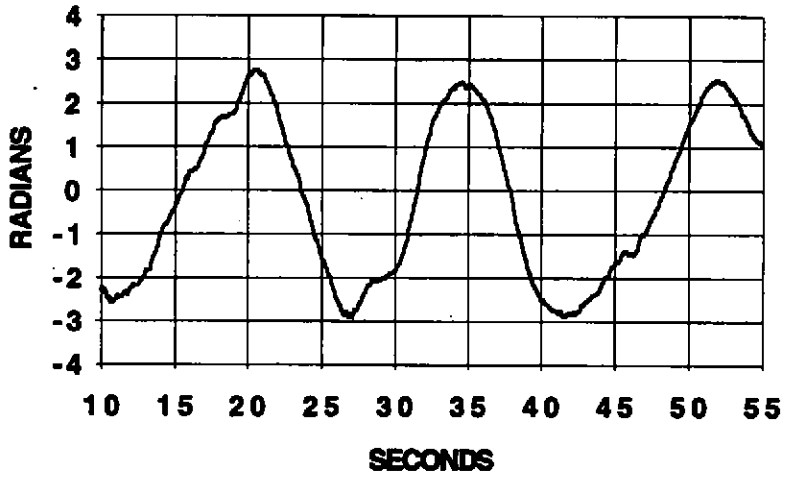

Figure 10: Phase record for 1100 Hz CW pulse.